Vitamin D receptor regulates high-level glucose induced retinal ganglion cell damage through STAT3 pathway

X.-J. LEI¹, Y.-L. XU¹, Y.-Q. YANG¹, Y.-W. BING¹, Y.-X. ZHAO²

Abstract. – OBJECTIVE: To explore the protective role of Vitamin D Receptor (VDR) in retinal ganglion cells (RGCs) after high-level glucose induction, and to investigate its underlying mechanism.

MATERIALS AND METHODS: Primary RGCs were isolated from 24-hour-old Sprague Dawley (SD) rats and cultured in 50 mmol/L glucose. The expression of VDR in RGCs induced by 50 mmol/L glucose at different time points was determined by Real-time quantitative polymerase chain reaction (qRT-PCR) and Western blot, respectively. Subsequently, VDR siRNA was transfected into RGCs. Transfection efficiency was determined by qRT-PCR and Western blot, respectively. The protein expressions levels of VDR, signal transducer and activator of transcription 3 (STAT3) and p-STAT3 in RGCs after VDR knockdown were determined by Western blot. MTT (3-(4,5-dimethylthiazol-2-yl)-2,5-diphenyl tetrazolium bromide) and cell counting kit-8 (CCK-8) assay were conducted to access the viability of RGCs after high-level glucose induction. Ki-67 staining was performed to detect the proliferation of RGCs. Meanwhile, the apoptosis of RGCs was evaluated by using Annexin-V FITC/PI and TUNEL (terminal dexynucleotidyl transferase(TdT)-mediated dUTP nick end labeling) assay, respectively. In addition, caspase-3 activity in RGCs was detected by relative commercial kit.

RESULTS: After 4 days of high-level glucose induction, the viability of RGCs was remarkably decreased. VDR was highly expressed in RGCs during high-level glucose culture. The mRNA and protein expression levels of VDR were both significantly downregulated after the transfection of VDR siRNA in RGCs. Meanwhile, VDR knockdown in RGCs significantly increased the viability and proliferative ability of RGCs, whereas significantly decreased apoptotic rate and caspase-3 activity. In addition, the protein level of p-STAT3 in RGCs was remarkably downregulated after VDR knockdown.

CONCLUSIONS: Inhibition of VDR exerts a protective role in high-level glucose induced RGCs damage by activating the STAT3 pathway.

Key Words:

DR, VDR, RGCS, STAT3, Small interfering RNA (SiR-NA).

Introduction

Diabetic retinopathy (DR) is one of the important causes of visual impairment and blindness. Recent studies¹ have shown that diabetes mellitus is the leading cause of DR, which is related to cell apoptosis resulted from retinal oxidative stress. As the main complication of diabetes, DR lacks effective treatment currently. Previous studies on the pathogenesis of DR have mainly focused on retinal capillary microcirculation. In recent years, retinal nerve tissues, such as retinal ganglion cells (RGCs), have gradually gained widespread attention in the pathological researches of DR². Vitamin D receptor (VDR) exists in a variety of cells and participates in the metabolism of calcium and phosphorus in the body. VDR regulates the transcription and expressions of various genes in cells, eventually affecting intracellular signal transductions related to inflammatory response, immune regulation and proteinuria production³⁻⁵. Researches have shown that VDR knockout in diabetic mice results in a sharp reduction in the number of podocytes in kidney tissue. Meanwhile, the pathological symptoms mainly include proteinuria and glomerular sclerosis⁶. To date, the role of VDR in high-level glucose induced damage of RGC has rarely been reported. Signal transducer and activator of transcription 3 (STAT3) is a member of the STATs family, which

¹Department of Ophthalmology, The Second Affiliate Hospital of Dalian Medical University, Dalian, China

²Department of Ophthalmology, Center hospital in Cangzhou, Cangzhou, China

is also an important signal transduction pathway in cells. After STAT3 phosphorylation, it forms a dimer and further transfers to the nucleus. It has been shown that nuclear STAT3 is capable of regulating the transcription and expression of multiple genes, thereafter affecting cell growth and apoptosis⁷. Moreover, the phosphorylation level of STAT3 is abnormally elevated in kidney tissues of patients with diabetic nephropathy, which is also found to be highly expressed in podocytes after high-level glucose induction. Therefore, the aim of this study was to explore the molecular mechanism of STAT3 in RGCs of high-level glucose damage by inhibiting VDR. Our study might provide a theoretical reference for the prevention and treatment of DR.

Materials and Methods

Reagents

Penicillin, streptomycin, Dulbecco's modified eagle medium/F12 (DMEM)/F12 and fetal bovine serum (FBS) were obtained from HyClone (South Logan, UT, USA); primary and secondary antibodies were obtained from Abcam (Cambridge, MA, USA); bicinchoninic acid (BCA) kit was obtained from Pierce (Rockford, IL, USA); TRIzol, complementary deoxyribose nucleic acid (cDNA) reverse transcription kit and SYBR Premix Ex Taq II were obtained from TaKaRa (Otsu, Shiga, Japan); MTT (3-(4,5-dimethylthiazol-2-yl)-2,5-diphenyl tetrazolium bromide) determination kit was obtained from Sangon (Shanghai, China); Ki-67 proliferation determination kit was obtained from Yutong (Jiangsu, China); ApopTag Plus Peroxidase In Situ Apoptosis Detection Kit was obtained from Chemicon (Millipore, Billerica, MA, USA).

Cell Culture of Primary RGCs

Cerebral stratum of the retina was harvested from 24-hour-old Sprague Dawley (SD) rats. Subsequently, collected tissues were washed with phosphate-buffered saline (PBS) containing 100 U/mL penicillin and 50 µg/mL streptomycin for four times. Tissues were then digested with 0.25% trypsin at 37°C for 25 min. The mixture was cultured in DMEM/F12 containing 10% FBS, 100 U/mL penicillin and 50 U/mL streptomycin. After centrifugation at 1200 r/min for 5 min, the cells were re-suspended in DMEM/F12 containing 10% FBS and seeded into 6-well plates pre-coated with OX-41. The culture medium was replaced

every 10 min, for a total of three times. The un-adherent cells were removed by washing with PBS for three times. As previously described, primary RGCs were induced with 50 mmol/L glucose for subsequent experiments. This study was approved by the Animal Ethics Committee of Dalian Medical University Animal Center.

Real-Time Quantitative Polymerase Chain Reaction (RT-qPCR)

Total RNA was extracted from RGCs according to the instructions of TRIzol reagent (Invitrogen, Carlsbad, CA, USA). Subsequently, extracted RNA was reversely transcribed into cDNA using the Primescript RT Reagent Kit (TaKaRa, Otsu, Shiga, Japan). Primers used in the study were as follows: VDR, forward: 5'-TCCTTCCTCTGCT-GGTAT-3', reverse: 5'-CTCCCTTGGTTAGTGT-GGTAG-3'; GAPDH, forward: 5'-CGTCTTCAC-CACCATGGAGA-3', reverse: 5'-CGGCCAT-CACGCCACAGTTT-3'. Relative gene expression was calculated by the 2-ΔΔCt method.

Western Blot

Total protein was extracted by radio-immunoprecipitation assay (RIPA) solution (Beyotime, Shanghai, China). The concentration of extracted protein was detected by the bicinchoninic acid (BCA) protein assay kit (Pierce Biotechnology, Rockford, IL, USA). Subsequently, equal amounts of protein samples were separated by sodium dodecyl sulphate-polyacrylamide gel electrophoresis (SDS-PAGE) and transferred onto polyvinylidene difluoride (PVDF) membranes (Millipore, Billerica, MA, USA). After blocking with 5% skimmed milk for 1 hour, the membranes were incubated with specific primary antibody at 4°C overnight. After washing with 1× Tris-buffered with Saline-Tween 20 (TBST) for 5 times (6 min for each time), the membranes were incubated with corresponding secondary antibody at room temperature for 2 h. After washing with 1×TBST for 1 min, immuno-reactive bands were exposed by the enhanced chemiluminescence method. Image-Pro Plus 6.0 Imaging System (Silver Springs, MD, USA) was used for analyzing the blot results.

Transfection

RGCs were first seeded in 6-well plates. Subsequently, 6 μL Turbofect containing VDR siR-NA/non-specific siRNA and 200 μL serum-free DMEM/F12 were added in each well for overnight cell culture.

MTT Assay

Transfected RGCs were seeded into 96-well plates at a density of 5×10^4 cells per well. 20 μL MTT solution (5 g/L) were added in each well, followed by incubation for 5 h. Subsequently, the culture medium was replaced with 150 μL dimethyl sulfoxide (DMSO) (Sigma-Aldrich, St. Louis, MO, USA) and gently mixed. Optical density (OD) value at the wavelength of 490 nm was measured by using a microplate reader.

Cell Counting Kit-8 (CCK-8) Assay

Transfected RGCs were seeded into 96-well plates at a density of 5×10^3 cells per well. After culture for 24 h, 10 μ L CCK-8 (Dojindo Laboratories, Kumamoto, Japan) solution were added in each well and incubated for 2 h. Finally, OD value at the wavelength of 490 nm was measured by using a microplate reader.

Ki-67 Staining

As described previously, RGCs were collected by Ki-67 staining for proliferation detection. Nucleus were stained with Hoechst 33342 (10 μ g/mL). RGCs were finally observed by a fluorescence microscope.

Annexin-V FITC /PI staining

RGCs were pre-seeded into 6-well plates, washed with PBS twice, and re-suspended in the binding buffer in dark for 15 min. Cells were then incubated with 5 μ L Annexin V-fluorescein isothiocyanate (FITC) and 5 μ L Propidium Iodide (PI) in dark. Cell apoptosis was detected by flow cytometry.

TUNEL (Terminal Dexynucleotidyl Transferase(Tdt)-Mediated Dutp Nick end Labeling) Assay

RGCs were collected, and the apoptotic rate was detected by using the ApopTag Plus Peroxidase In Situ Apoptosis Detection Kit (Merck, Millipore, Billerica, MA, USA). Nucleus was stained with Hoechst 33342 (10 µg/mL). Apoptotic cells were observed under a fluorescence microscope.

Caspase-3 Activity Determination

RGCs were collected, and caspase-3 activity was determined in accordance with the instructions of BD ApoAlert Caspase-3 Fluorescent Assay Kit (BD Biosciences, Franklin Lakes, NJ, USA).

Statistical Analysis

Statistical Product and Service Solutions (SPSS) 16.0 Software (SPSS Inc., Chicago, IL, USA) was used for all statistical analysis. All data were expressed as $\bar{x}\pm s$. Independent sample t-test was performed to compare the differences between two groups. One-way ANOVA was used to compare the differences among different groups, followed by post-hoc test. p < 0.05 was considered statistically significant.

Results

VDR Was Highly Expressed In RGCs With High-Level Glucose Damage

Isolated RGCs were first cultured in DMEM/ F12 containing 50 mmol/L glucose, and then cell growth viability was determined at different time points. Results showed that the growth viability of RGCs was significantly decreased on the fourth day of culture (p < 0.05, Figure 1). Hence, RGCs cultured for 4 days in a high-level glucose environment were chosen for subsequent experiments. To determine whether VDR was involved in the regulation of high-level glucose-induced damage in RGCs, we detected its expression in RGCs after 4-days culture in high-level glucose environment. Interestingly, we found that both mRNA (Figure 2A) and protein (Figure 2B) expression levels of VDR were remarkably higher than those of normal controls, suggesting that VDR might be involved in the regulation of high-level glucose damage in RGCs.

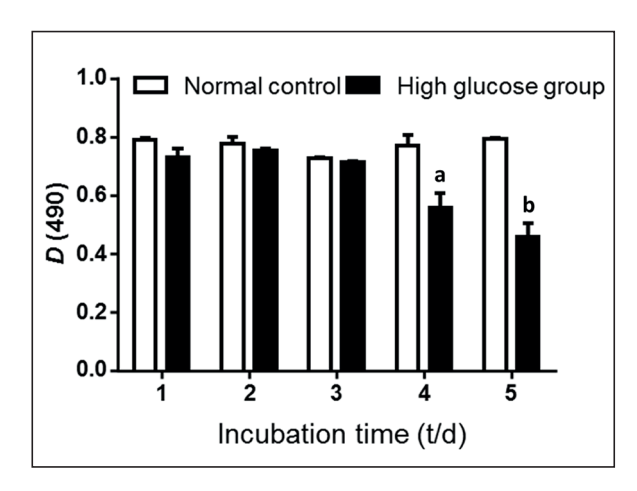


Figure 1. Effects of high-level glucose treatment on RGCs with different culture duration. Cell growth viability of RGCs cultured with 50 mmol/L glucose at different time points. a: p < 0.05, b: p < 0.01, compared with the control group.

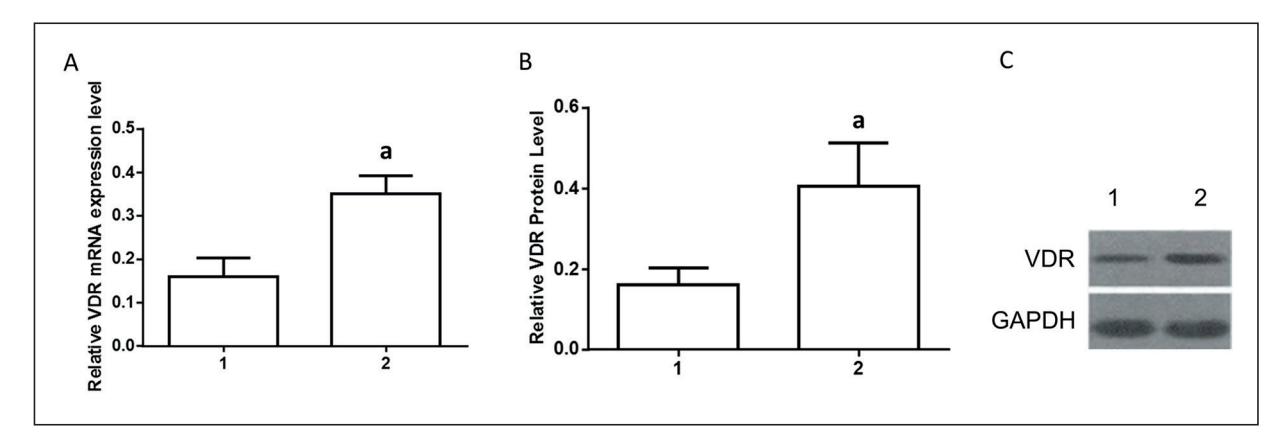


Figure 2. Effects of high-level glucose on VDR expression in RGCs. (A) The mRNA expression level of VDR. (B) Quantification of the protein expression level of VDR. (C) The protein level of VDR detected by Western blot. a: p < 0.05, compared with the control group (1: the control group; 2: the high-level glucose group).

VDR Knockdown in RGCs

To further determine the role of VDR in the regulation of RGCs with high-level glucose damage, we constructed a VDR knockdown model by transfecting VDR siRNA in RGCs. Transfection efficiency of VDR siRNA was detected by qRT-PCR and Western blot, respectively. Results indicated that both mRNA (Figure 3A) and protein (Figure 3B) levels of VDR were significantly decreased after transfection of VDR siRNA (p < 0.05). According to the mRNA levels of VDR in the siRNA group and the control group, the transfection efficiency of VDR siRNA was up to 52%.

VDR Knockdown Attenuated Inhibited Growth and Proliferation of RGCs Induced by High-Level Glucose Damage

To access the effects of VDR on the biological properties of RGCs after high-level glucose treatment, the growth viability and proliferative ability of RGCs were determined by MTT, CCK-8 assay and Ki-67 staining, respectively. Experimental results showed that both the growth viability (Figure 4A) and proliferative ability (Figure 4B) of the VDR si-RNA group were significantly increased when compared with those of the non-specific siRNA group and the control group

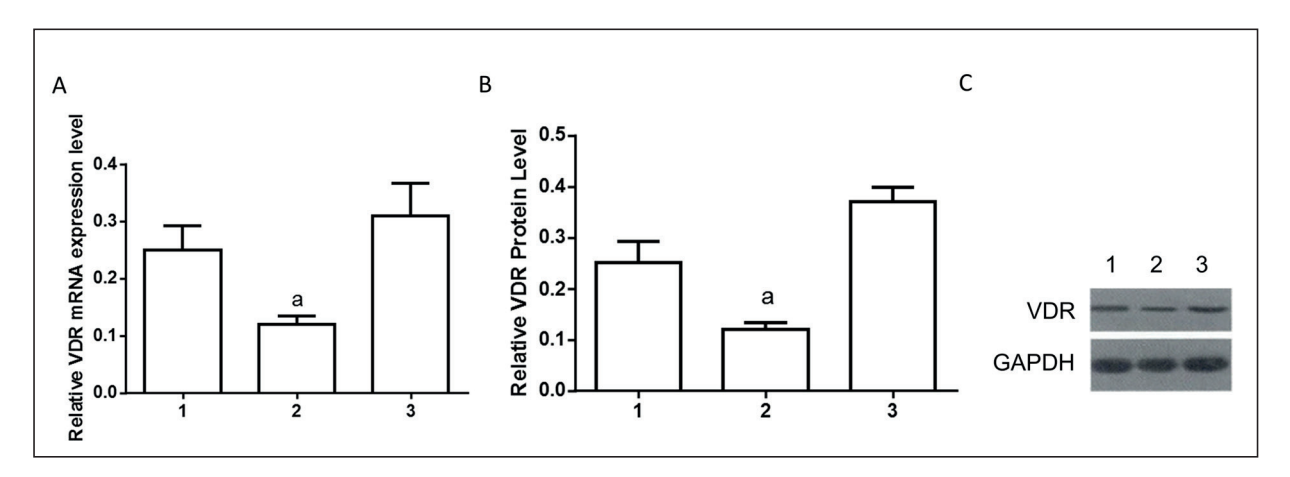


Figure 3. VDR expression in RGCs after transfection. (A) The mRNA expression level of VDR after transfection. (B) Quantification of the protein expression level of VDR after transfection. (C) The protein level of VDR detected by Western blot after transfection. a: p < 0.05, compared with the non-specific siRNA group (1: the control group; 2: the VDR siRNA group; 3: the non-specific siRNA group).

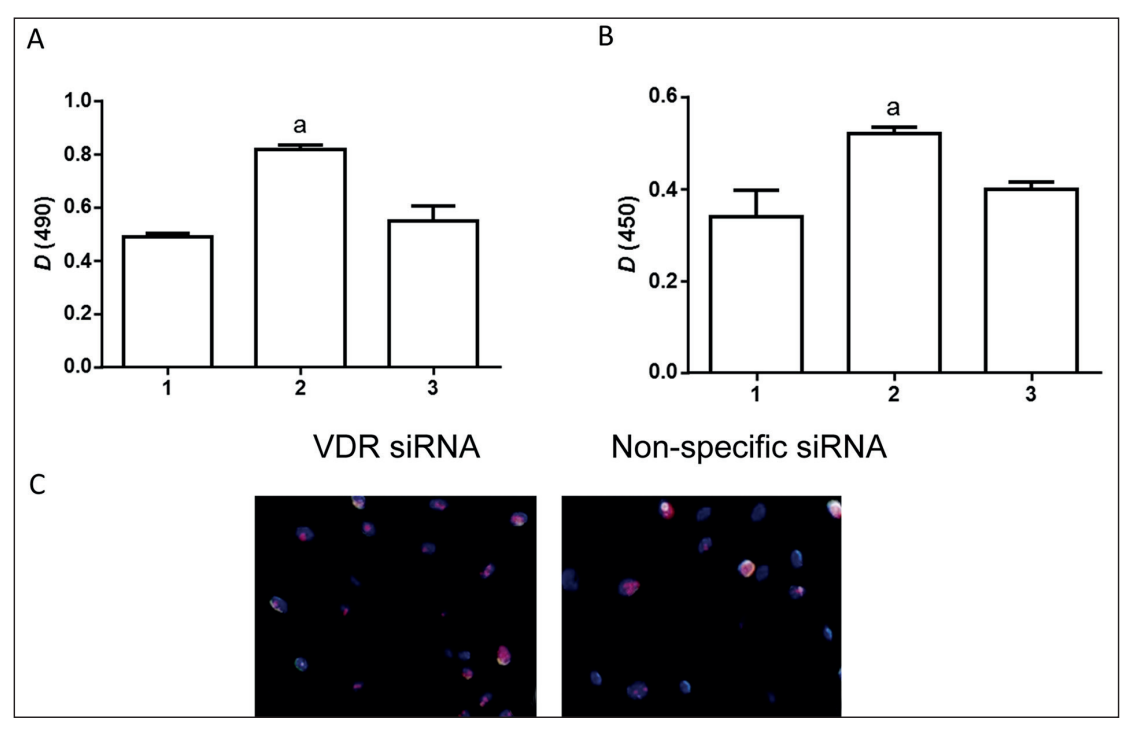


Figure 4. Effects of VDR knockdown on the viability and proliferation of RGCs. (*A*) Cell viability of RGCs after VDR knockdown. (*B*) Cell proliferation of RGCs after VDR knockdown. (*C*) Ki-67 staining of RGCs after VDR knockdown (magnification $400\times$). Ki-67 staining (red) and Hoechst 33342 staining of cell nucleus (blue) in the VDR siRNA group and the non-specific siRNA group. a: p < 0.05, compared with the non-specific siRNA group (1: the control group; 2: the VDR siRNA group; 3: the non-specific siRNA group).

(p < 0.05). In addition, compared with the non-specific siRNA group (Figure 4C-right), higher positive expression of Ki-67 staining was observed in the VDR siRNA group (Figure 4C-left). These findings all suggested that VDR knockdown could alleviate the inhibitory effects of high-level glucose on the growth and proliferation of RGCs.

VDR Knockdown Decreased the Apoptosis of RGCs Induced by High-Level Glucose Damage

To explore the specific role of VDR in the apoptosis of RGCs after high-level glucose treatment, we detected caspase-3 activity and the apoptotic rate by Annexin-VFITC /PI staining and TUNEL assay, respectively. We found that caspase-3 activity (Figure 5A) and the apoptotic rate (Figure 5B) in the VDR si-RNA group were remarkably decreased when compared with those of the non-specific siRNA group and the control group (p < 0.05). TUNEL assay showed that less apoptotic RGCs were found in the VDR si-RNA group than the non-specific siRNA group (Figure 5C). Therefore, we believed that VDR knock-

down could significantly decrease the apoptotic rate of RGCs induced by high-level glucose damage.

VDR Knockdown Inhibited STAT3 Pathway

Previous studies have pointed out that activation of the STAT3 pathway promotes cell apoptosis. In the present study, we detected the protein level of phosphorylated STAT3 in RGCs by Western blot, and further verified whether STAT3 was involved in high-level glucose damage in RGCs. Compared with the non-specific siRNA group and the control group, the expression level of phosphorylated STAT3 was remarkably downregulated in the VDR si-RNA group (Figure 6, p < 0.01). Our data demonstrated that STAT3 pathway was related to high-level glucose damage in RGCs and was inhibited after VDR knockdown.

Discussion

Diabetes mellitus is a kind of metabolic disease caused by disordered insulin secretion and

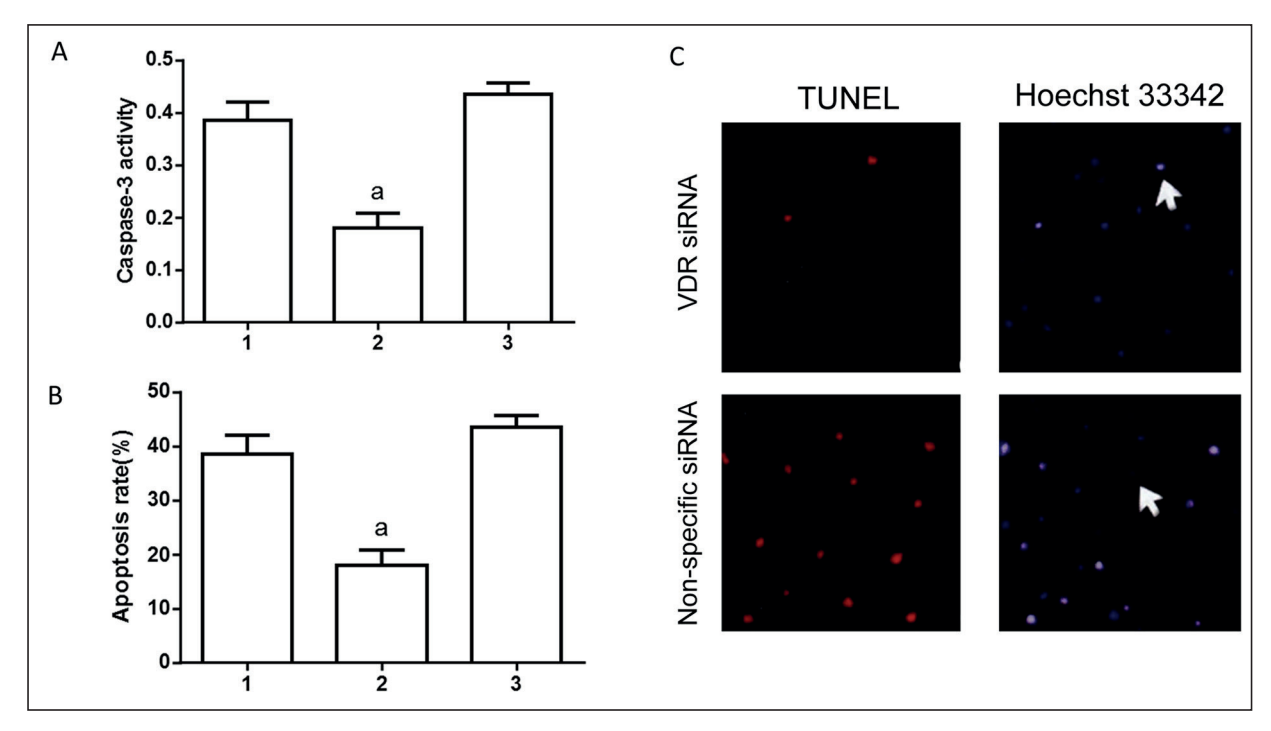


Figure 5. Effects of VDR knockdown on caspase-3 activity and the apoptosis of RGCs. (*A*) Caspase-3 activity of RGCs after VDR knockdown. (*B*) Cell apoptosis of RGCs after VDR knockdown. (*C*) TUNEL staining (red) of RGCs after VDR knockdown; Hoechst 33342 staining was performed to indicate the nucleus (blue) (200×). Arrow indicated apoptotic cells. a: p < 0.01, compared with the non-specific siRNA group (1: the control group; 2: the VDR siRNA group; 3: the non-specific siRNA group).

function. Hyperglycemia induced by diabetes can lead to long-term damage to different organs, including eyes, kidneys, nerves, heart and blood vessels^{8,9}. As one of the most common complications of diabetes, DR can even cause blindness. With the rapid changes in living standards and

lifestyles, the incidence of diabetes increases year by year. Meanwhile, the incidence of DR is also on the rise. However, current treatment fails to cure DR effectively. In this study, we investigated the protective effect of VDR on RGCs induced by high-level glucose *in vitro*. The aim of this

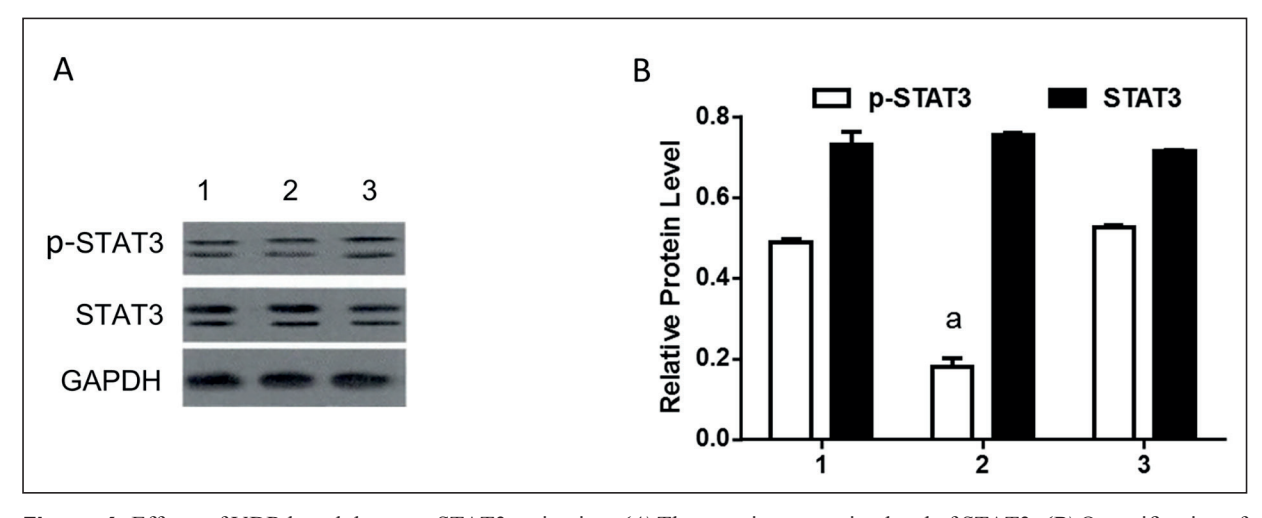


Figure 6. Effects of VDR knockdown on STAT3 activation. (A) The protein expression level of STAT3. (B) Quantification of the protein expression level of STAT3. a: p < 0. 05, compared with the non-specific siRNA group (1: the control group; 2: the VDR siRNA group; 3: the non-specific siRNA group).

study was to provide a new theoretical reference for the prevention and treatment of DR. Vitamin D is reported to be involved in the development and progression of chronic kidney diseases. The deficiency of vitamin D is also associated with the development of diabetic nephropathy. Meanwhile, administration of vitamin D drugs can effectively reduce the ratio of urinary albumin and creatinine level in patients with chronic kidney diseases. VDR is a transcriptional regulator that specifically binds to vitamin D metabolites, which may serve as a receptor for vitamin D. Recent studies^{10,11} have shown that VDR is widely expressed in kidney tissues, and is also found in glomerular epithelial cells, podocytes as well as juxtaglomerular apparatus. Previous studies have reported abnormal upregulation of angiotensin and renin levels in VDR-/- diabetic mice. These mice exhibit severe renal tissue damage, accompanied by other symptoms such as renal interstitial fibrosis and proteinuria. Meanwhile, abundant podocyte apoptosis has been observed in kidney tissue of these mice¹². In the present work, we found that VDR was highly expressed in RGCs extracted from rats with high-level glucose damage. VDR knockdown remarkably enhanced the survival rate of RGCs, whereas decreased the apoptotic rate and caspase-3 activity in RGCs. Therefore, we believed that VDR inhibition could protect RGCs from high-level glucose damage. As an important member of the JAK-STAT pathway, STAT3 exerts an essential role in regulating cell proliferation, survival, apoptosis and differentiation. In vitro experiments have confirmed that STAT3 can be activated by a variety of stimuli, including angiotensin II, high-level glucose, interleukin-6 and oxidative stress¹³⁻¹⁶. Meanwhile, the STAT3 pathway can be observed in various animal models, such as diabetic nephropathy, Thy1-1 glomerulonephritis, ischemia-reperfusion nephropathy, obstructive nephropathy, and human immunodeficiency virus (HIV)-associated nephropathy¹⁷. Clinical studies have reported that activated phosphorylation of STAT3 pathway can be detected by renal biopsy in patients with diabetic nephropathy, IgA nephropathy, lupus nephropathy, and vasculitis¹⁸. Inhibition of phosphorylated STAT3 may improve renal function and reduce renal tissue inflammation in rats with diabetic nephropathy. Moreover, it is believed that phosphorylation of the STAT3 pathway plays an essential role in the pathogenesis of diabetes, which can be applied as an intervention target for diabetes treatment. In the present research, VDR

knockdown in RGCs remarkably downregulated the level and activity of phosphorylated STAT3. We concluded that VDR could protect RGCs from high-level glucose damage via regulating the STAT3 pathway. Caspase-3 is a homologous cysteine protease involved in the process of apoptosis, which is also considered as an activator of apoptosis¹⁹. Activated intracellular death signals stimulate the activation of caspase-3, in turn initiating the hydrolysis of target proteins, such as cytoskeletal proteins. This may eventually promote cell apoptosis²⁰. In this experiment, lowly expressed VDR, decreased STAT3 activation and caspase-3 activity were observed in RGCs of high-level glucose damage. In summary, we found that high-level glucose damage in RGCs resulted in the upregulation of VDR expression. Knockdown of VDR significantly promoted cell growth and proliferation. Meanwhile, VDR down-regulation remarkably inhibited caspase-3 activity and apoptosis in impaired RGCs, indicating the protective effect of VDR inhibition on RGCs. Additionally, inhibition of VDR downregulated STAT3 phosphorylation. This further suggested that inhibition of VDR might protect RGCs from high-level glucose damage by regulating the STAT3 pathway. Therefore, VDR can be used as a potential target molecule for DR prevention, providing a new speculative basis for the prevention and treatment of DR.

Conclusions

Inhibition of VDR expression exerts a protective role in high-level glucose damage induced RGCs by activating the STAT3 pathway.

Conflict of Interest

The Authors declare that they have no conflict of interests.

References

YAU JW, ROGERS SL, KAWASAKI R, LAMOUREUX EL, KOWALSKI JW, BEK T, CHEN SJ, DEKKER JM, FLETCHER A, GRAUSLUND J, HAFFNER S, HAMMAN RF, IKRAM MK, KAYAMA T, KLEIN BE, KLEIN R, KRISHNAIAH S, MAYURASAKORN K, O'HARE JP, ORCHARD TJ, PORTA M, REMA M, ROY MS, SHARMA T, SHAW J, TAYLOR H, TIELSCH JM, VARMA R, WANG JJ, WANG N, WEST S, XU L, YASUDA M, ZHANG X, MITCHELL P, WONG TY. Global prevalence and major risk factors of diabetic retinopathy. Diabetes Care 2012; 35: 556-564.

- 2) VAN DIJK HW, VERBRAAK FD, STEHOUWER M, KOK PH, GARVIN MK, SONKA M, DEVRIES JH, SCHLINGEMANN RO, ABRAMOFF MD. Association of visual function and ganglion cell layer thickness in patients with diabetes mellitus type 1 and no or minimal diabetic retinopathy. Vision Res 2011; 51: 224-228.
- 3) VEDRALOVA M, KOTRBOVA-KOZAK A, ZELEZNIKOVA V, ZOUBKOVA H, RYCHLIK I, CERNA M. Polymorphisms in the vitamin D receptor gene and parathyroid hormone gene in the development and progression of diabetes mellitus and its chronic complications, diabetic nephropathy and non-diabetic renal disease. Kidney Blood Press Res 2012; 36: 1-9.
 - 4) THILL M, BECKER S, FISCHER D, CORDES T, HORNEMANN A, DIEDRICH K, SALEHIN D, FRIEDRICH M. Expression of prostaglandin metabolising enzymes COX-2 and 15-PGDH and VDR in human granulosa cells. Anticancer Res 2009; 29: 3611-3618.
- CADARIO F, SAVASTIO S, RIZZO AM, CARRERA D, BONA G, RICORDI C. Can Type 1 diabetes progression be halted? Possible role of high dose vitamin D and omega 3 fatty acids. Eur Rev Med Pharmacol Sci 2017; 21: 1604-1609.
- 6) SANCHEZ-NINO MD, BOZIC M, CORDOBA-LANUS E, VALCHEVA P, GRACIA O, IBARZ M, FERNANDEZ E, NAVARRO-GONZALEZ JF, ORTIZ A, VALDIVIELSO JM. Beyond proteinuria: VDR activation reduces renal inflammation in experimental diabetic nephropathy. Am J Physiol Renal Physiol 2012; 302: F647-F657.
- TANG SC, YIU WH, LIN M, LAI KN. Diabetic nephropathy and proximal tubular damage. J Ren Nutr 2015; 25: 230-233.
- RAINS JL, JAIN SK. Oxidative stress, insulin signaling, and diabetes. Free Radic Biol Med 2011; 50: 567-575.
- LIU DH, YUAN FG, HU SQ, DIAO F, WU YP, ZONG YY, SONG T, LI C, ZHANG GY. Endogenous nitric oxide induces activation of apoptosis signal-regulating kinase 1 via S-nitrosylation in rat hippocampus during cerebral ischemia-reperfusion. Neuroscience 2013; 229: 36-48.
- 10) SANTORO D, CACCAMO D, GAGLIOSTRO G, IENTILE R, BEN-VENGA S, BELLINGHIERI G, SAVICA V. Vitamin D metabolism and activity as well as genetic variants of the vitamin D receptor (VDR) in chronic kidney disease patients. J Nephrol 2013; 26: 636-644.
- 11) Uchiyama T, Tatsumi N, Kamejima S, Waku T, Ohkido I, Yokoyama K, Yokoo T, Okabe M. Hypermethyla-

- tion of the CaSR and VDR genes in the parathyroid glands in chronic kidney disease rats with high-phosphate diet. Hum Cell 2016; 29: 155-161.
- GLENN DJ, CARDEMA MC, GARDNER DG. Amplification of lipotoxic cardiomyopathy in the VDR gene knockout mouse. J Steroid Biochem Mol Biol 2016; 164: 292-298.
- 13) AMIRI F, SHAW S, WANG X, TANG J, WALLER JL, EATON DC, MARRERO MB. Angiotensin II activation of the JAK/STAT pathway in mesangial cells is altered by high glucose. Kidney Int 2002; 61: 1605-1616.
- 14) Wang X, Shaw S, Amiri F, Eaton DC, Marrero MB. Inhibition of the Jak/STAT signaling pathway prevents the high glucose-induced increase in tgf-beta and fibronectin synthesis in mesangial cells. Diabetes 2002; 51: 3505-3509.
- 15) LEE YJ, HEO JS, SUH HN, LEE MY, HAN HJ. Interleukin-6 stimulates alpha-MG uptake in renal proximal tubule cells: involvement of STAT3, PI3K/Akt, MAPKs, and NF-kappaB. Am J Physiol Renal Physiol 2007; 293: F1036-F1046.
- 16) ARANY I, MEGYESI JK, NELKIN BD, SAFIRSTEIN RL. STAT3 attenuates EGFR-mediated ERK activation and cell survival during oxidant stress in mouse proximal tubular cells. Kidney Int 2006; 70: 669-674.
- 17) BARTON BE, KARRAS JG, MURPHY TF, BARTON A, HUANG HF. Signal transducer and activator of transcription 3 (STAT3) activation in prostate cancer: direct STAT3 inhibition induces apoptosis in prostate cancer lines. Mol Cancer Ther 2004; 3: 11-20.
- 18) Kordula T, Bugno M, Goldstein J, Travis J. Activation of signal transducer and activator of transcription-3 (Stat3) expression by interferon-gamma and interleukin-6 in hepatoma cells. Biochem Biophys Res Commun 1995; 216: 999-1005.
- 19) SUFFERT G, MALTERER G, HAUSSER J, VIILIAINEN J, FENDER A, CONTRANT M, IVACEVIC T, BENES V, GROS F, VOINNET O, ZAVOLAN M, OJALA PM, HAAS JG, PFEFFER S. Kaposi's sarcoma herpesvirus microRNAs target caspase 3 and regulate apoptosis. PLoS Pathog 2011; 7: e1002405.
- 20) FANG J, SONG XW, TIAN J, CHEN HY, LI DF, WANG JF, REN AJ, YUAN WJ, LIN L. Overexpression of microR-NA-378 attenuates ischemia-induced apoptosis by inhibiting caspase-3 expression in cardiac myocytes. Apoptosis 2012; 17: 410-423.